

## **Supplementary Information**

### **Identification of the First Highly Selective inhibitor of Human Lactate Dehydrogenase B**

Sachio Shibata<sup>1+\*</sup>, Satoshi Sogabe<sup>1#</sup>, Masanori Miwa<sup>1</sup>, Takuya Fujimoto<sup>2</sup>, Nobuyuki Takakura<sup>2</sup>, Akihiko Naotsuka<sup>1</sup>, Shuji Kitamura<sup>2</sup>, Tomohiro Kawamoto<sup>1\*</sup>, and Tomoyoshi Soga<sup>3</sup>

Supplemental Data includes:

Supplementary Figure 1. Linearity of MS-based NADH and NAD<sup>+</sup> detection.

Supplementary Figure 2. Determination of LDHB and LDHA assay conditions.

Supplementary Figure 3. Nonlinear fits of the Michaelis–Menten kinetics for LDHB in the presence of AXKO-0046.

Supplementary Figure 4. Time-dependency inhibition of LDHB activity by AXKO-0046.

Supplementary Figure 5. The F<sub>obs</sub>–F<sub>calc</sub> electron density omit maps of the quarterly complex contoured at 3 $\sigma$

Supplementary Figure 6. Superposition of eight monomers in the asymmetric unit of the LDHB/NADH complex.

Supplementary Figure 7. Comparison of the root-mean-square deviation values per amino-acid residue of LDHB between the two complexes.

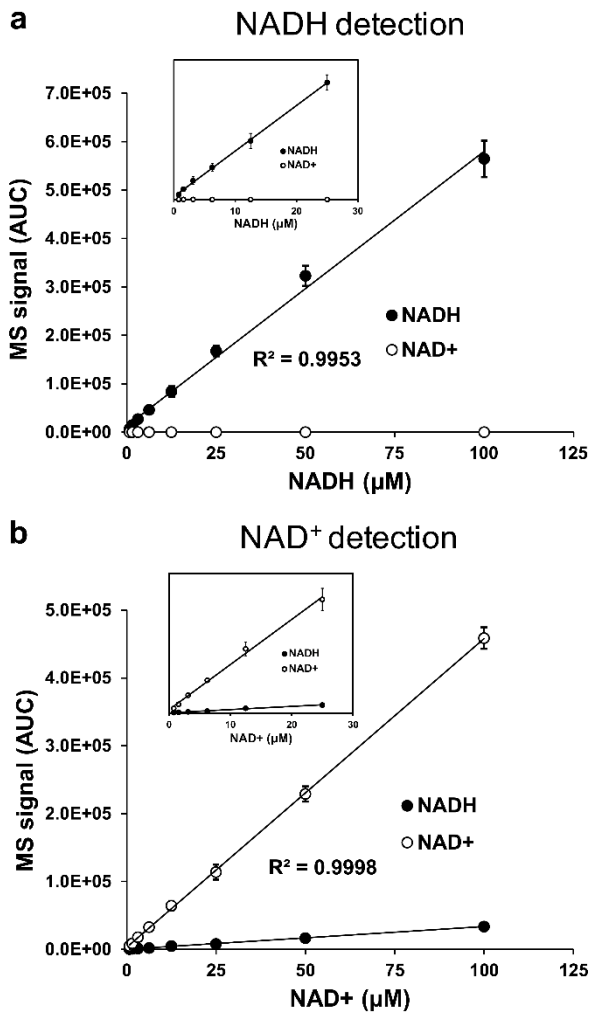
Supplementary Figure 8. Sequence alignment of human LDHA and human LDHB.

Supplementary Figure 9. Structural comparison between the allosteric site of LDHB and that of LDHA (PDB code 4OKN).

Supplementary Table 1. Selectivity profile of the LDHB hit compound.

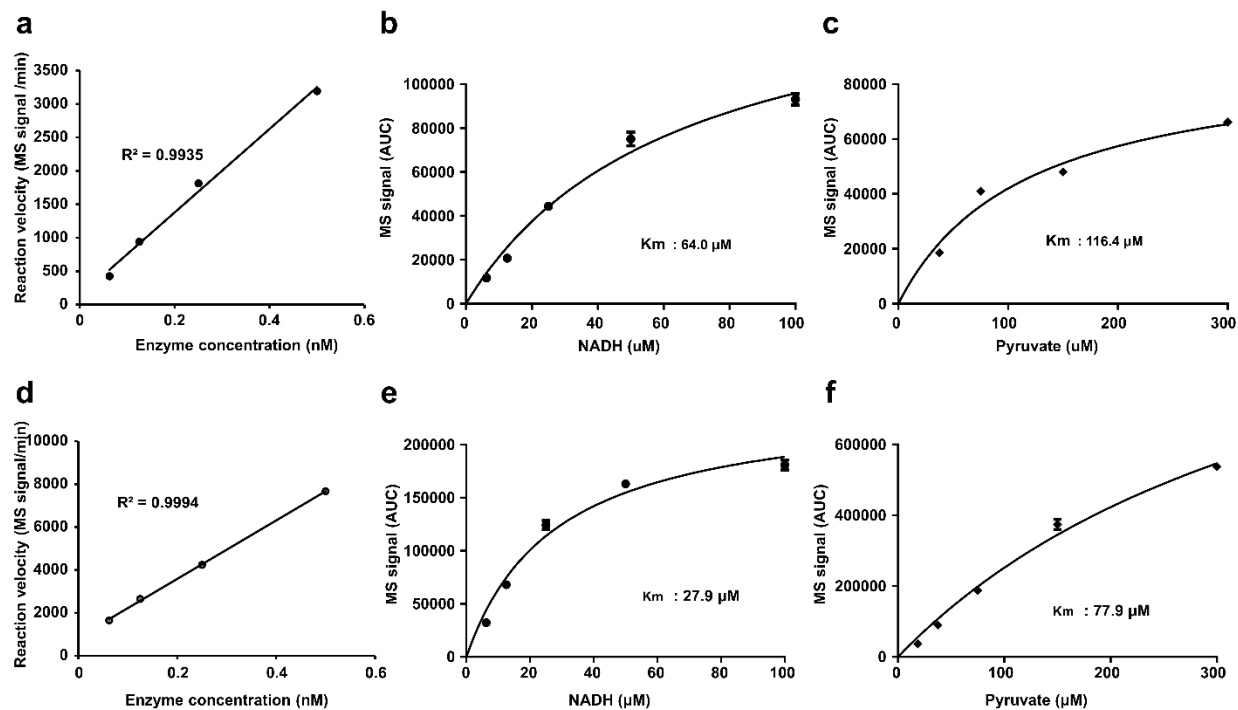
Supplementary Table 2. Inhibitory activity of LDHB by AXKO-0046 at varying concentrations of NADH and pyruvate.

Supplementary Table 3. Data collection and refinement statistics.



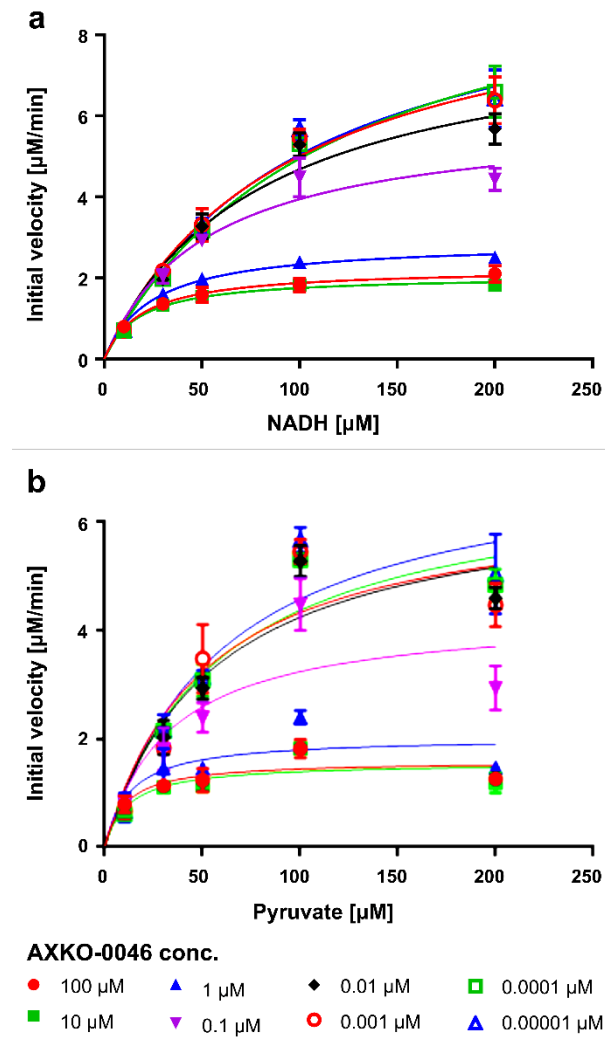
**Supplementary Figure 1. Linearity of MS-based NADH and NAD<sup>+</sup> detection.**

Linearity were detected up to 100  $\mu\text{M}$  NADH, **a** (closed circles) and NAD<sup>+</sup>, **b** (open circles) with a limit of detection at 0.78  $\mu\text{M}$  using the RF-MS assay. Linearity is shown as insets for lower concentrations of the analytes. Data shown are mean  $\pm$  standard deviation (SD) ( $n=4$ ).

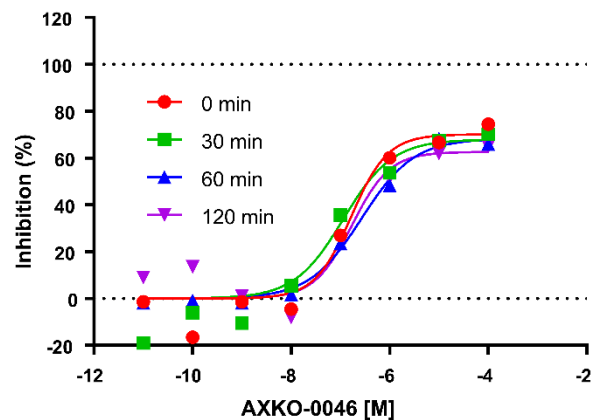


**Supplementary Figure 2. Determination of LDHB and LDHA assay conditions.**

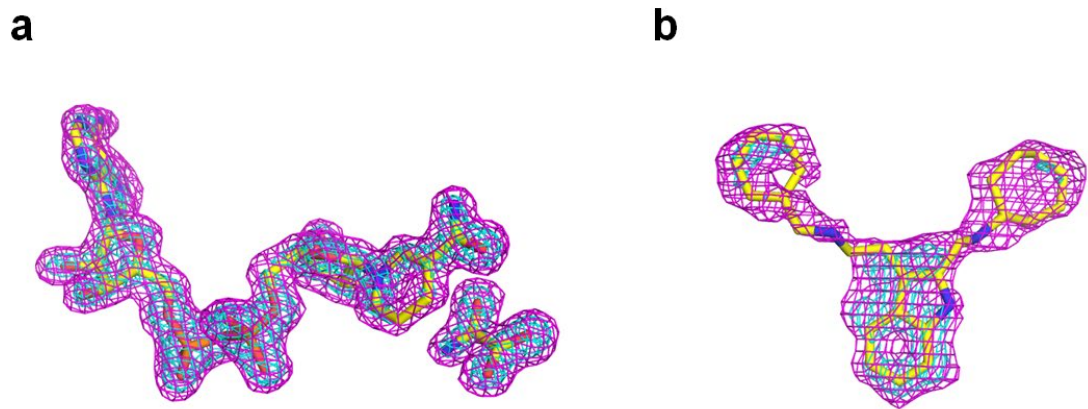
**a, d** Initial velocities for LDHB with pyruvate (75 μM) and NADH (75 μM) determined using RapidFire MS. The LDHB or LDHA reaction (0.0625 to 0.5 nM) showed good linearity up to 20 min. The assay was performed with pyruvate (500 μM) and increasing concentrations of NADH, **b, e** or NADH (500 μM) and increasing concentrations of pyruvate **c, f**. Data were fitted to the Michaelis–Menten equations to obtain kinetic constants Km using GraphPad Prism. Data are shown as the mean ± standard deviation (SD) ( $n=4$ ).



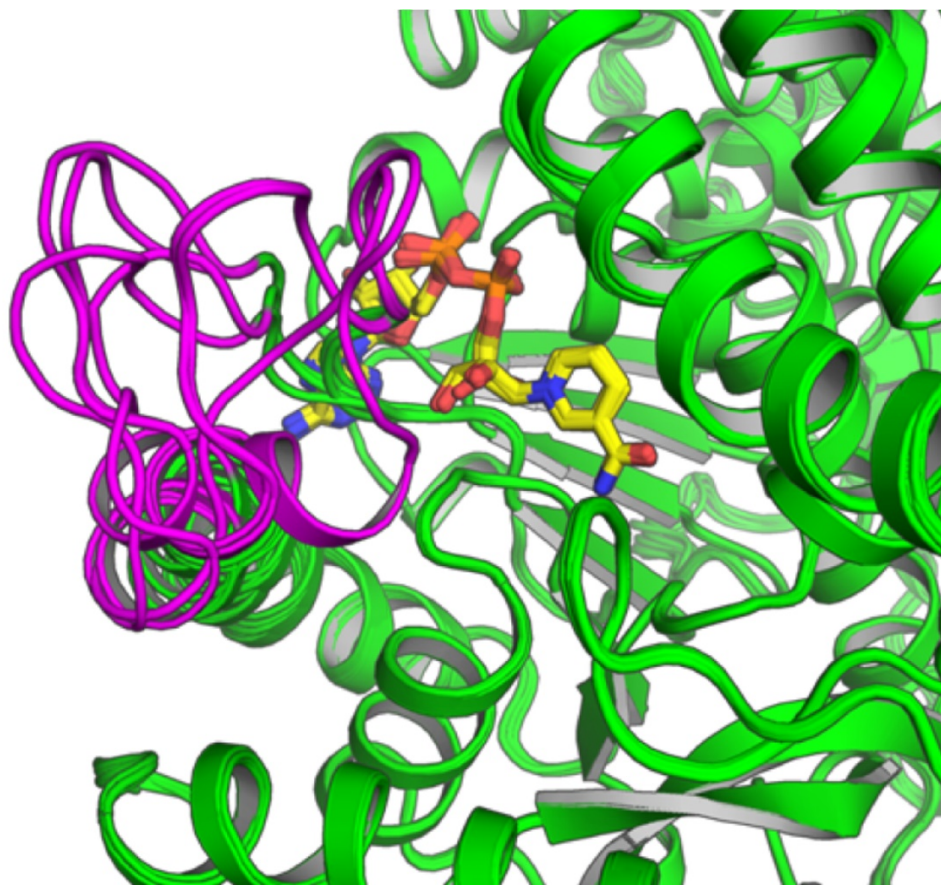
**Supplementary Figure 3. Nonlinear fits of the Michaelis–Menten kinetics for LDHB in the presence of AXKO-0046.** Michaelis-Menten Kinetics for LDHB were determined from the initial reaction velocities of **a** NADH and **b** pyruvate of varying substrate concentrations in the presence of the indicated concentration of AXKO-0046



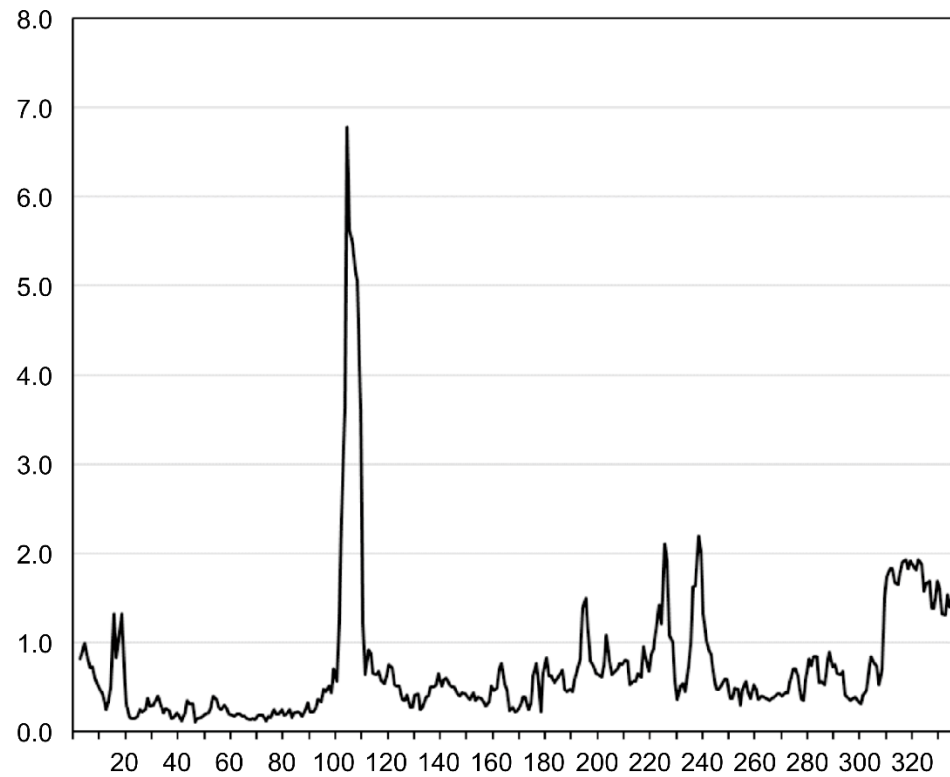
**Supplementary Figure 4. Time-dependency inhibition of LDHB activity by AXKO-0046.** Time dependency inhibition was measured by preincubating AXKO-0046 and LDHB for 0, 30, 60 or 120 min as indicated before initiating the LDHB reaction. Data are shown as the mean ( $n=2$ ).



**Supplementary Figure 5. The  $F_{\text{obs}} - F_{\text{calc}}$  electron density omit maps of the quarterly complex contoured at  $3\sigma$ : a NADH and oxamate and b AXKO-0046.**



**Supplementary Figure 6. Superposition of eight monomers in the asymmetric unit of the LDHB/NADH complex.** The active-site loop (residues Glu101–Leu110) is in magenta.

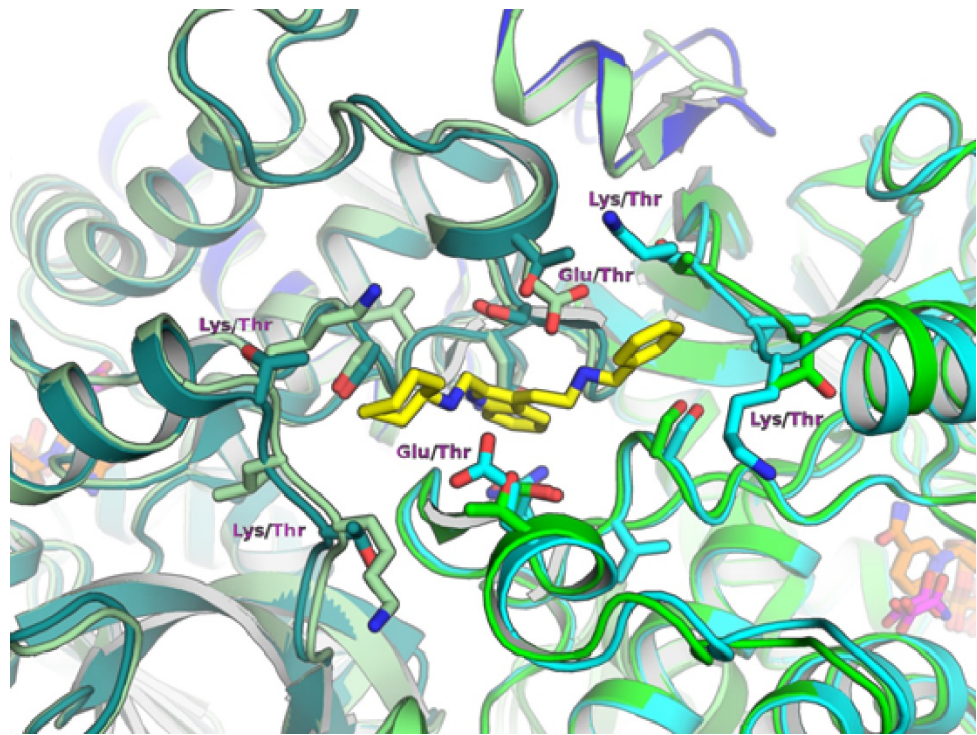


**Supplementary Figure 7. Comparison of the root-mean-square deviation values per amino-acid residue of LDHB between the two complexes.** RMSD was calculated from the sets of aligned conformations.

LDHA	1	MATLK DQLIY	NLLKEEQT - P	QNKITVVGVG	AVGMACAI SI	LMKDLA DELA	LVDVIEDKLK	59
LDHB	1	MATLK EKLIA	PVAEEEATVP	NNKITVVGVG	QVGMACAI SI	LGKSLA DELA	LVDVLEDKLK	60
LDHA	60	GEMMDLQHGS	LFLRTPKIVS	GKDYNVTANS	KLVII TAGAR	QQEGESRLNL	VQRNVNI FKF	119
LDHB	61	GEMMDLQHGS	LFLQTPKIVA	DKDYSVTANS	KIVVVTAGVR	QQEGESRLNL	VQRNVNV FKF	120
LDHA	120	IIPNVVKYSP	NCKLLIVSNP	VDILTYVAWK	ISGFPKNRVI	GSGCNLDSAR	FRYLMGERLG	179
LDHB	121	IIPQIVVKYSP	DCIIIVVSNP	VDILTYVTWK	LSGLPKHRVI	GSGCNLDSAR	FRYLMMAEKLG	180
LDHA	180	VHPLSCHGWV	LGEHGDSVP	VWSGMNVAGV	SLKTLHPDLG	TDKDKEQWKE	VHKQVVESAY	239
LDHB	181	IHPSSCHGWI	LGEHGDSVA	VWSGVNVAGV	SLQELNPEMG	TDNDSENWKE	VHKMVVESAY	240
LDHA	240	EVIKLKGYTS	WAIGL SVADL	AESIMKNLRR	VHPVSTMVK	LYGIKDDVFL	SVPCILGQNG	299
LDHB	241	EVIKLKGYTN	WAIGL SVADL	IESMLKNLSR	IHPVSTMVK	MYGIFNEVFL	SLPCILNARG	300
LDHA	300	ISDLVKVTLT	SEEEARLKKs	ADTLWGIQKE	LQ - F			332
LDHB	301	LTSVINQKLK	DDEVAQLKKs	ADTLWDIQKD	LKDL			334

### Supplementary Figure 8. Sequence alignment of human LDHA and human LDHB.

Residues depicted in Figure 5b are in red.



**Supplementary Figure 9. Structural comparison between the allosteric site of LDHB and that of LDHA (PDB code 4OKN).** Amino acid differences of both enzymes are labelled.

**Supplementary Table 1. Selectivity profile of the LDHB hit compound.**

ID	Deconvolution assay (% inhibition at 30 $\mu$ M)	LDHB (IC <sub>50</sub> , $\mu$ M)	LDHA (IC <sub>50</sub> , $\mu$ M)	Ratio (LDHA (IC <sub>50</sub> ) /LDHB (IC <sub>50</sub> ))
AXKO-0001	50	23	12	0.5
AXKO-0002	95	5.6	<3	<0.5
AXKO-0003	50	33	71	2.2
AXKO-0004	45	15	>300	20.0
AXKO-0005	38	32	34	1.1
AXKO-0006	37	30	6.4	0.21
AXKO-0007	40	38	28	0.7
AXKO-0008	53	16	130	8.1
AXKO-0009	54	21	39	1.9
AXKO-0010	44	<3	>300	>100
AXKO-0011	59	17	22	1.3
AXKO-0012	53	8.1	6.8	0.8
AXKO-0013	84	5.5	30	5.5
AXKO-0014	67	15	77	5.1
AXKO-0015	51	30	130	4.3
AXKO-0016	55	13	19	1.5
AXKO-0017	60	22	24	1.1
AXKO-0018	92	6.7	<3	<0.4
AXKO-0019	49	27	36	1.3
AXKO-0020	78	9.5	22	2.3
AXKO-0021	53	20	63	3.2
AXKO-0022	34	15	39	3.2

**Supplementary Table 2. Inhibitory activity of LDHB by AXKO-0046 at varying concentrations of NADH and pyruvate.**

	NADH (μM)				
	10	30	50	100	200
IC <sub>50</sub> (nM)	N.D.	702.1	329.5	223.0	94.2
	Pyruvate (μM)				
	10	30	50	100	200
IC <sub>50</sub> (nM)	N.D.	197.1	114.2	223.0	96.3

**Supplementary Table 3. Data collection and refinement statistics.**

	LDHB/NADH/oxamate/AXKO-0046	LDHB/NADH
<b>Data collection</b>		
Space group	$P2_1$	$C2$
Unit cell dimensions a, b, c (Å), $\alpha$ , $\beta$ , $\gamma$ (°)	59.4, 137.6, 84.9, 90, 109.3, 90	232.5, 84.2, 156.2, 90, 120.8, 90
Resolution (Å)	50-1.55 (1.58-1.55)	50-1.80 (1.83-1.80)
Redundancy	4.1 (3.5)	3.4 (3.4)
Completeness (%)	99.2 (93.8)	99.6 (100.0)
$I/\sigma$	20.3 (4.0)	19.8 (2.1)
$R_{\text{sym}}$	0.076 (0.251)	0.065 (0.511)
$CC_{1/2}$	0.989 (0.923)	0.994 (0.736)
<b>Refinement</b>		
Resolution (Å)	50-1.55 (1.58-1.55)	50-1.80 (1.85-1.80)
No. reflections	174218 (12517)	225765 (17284)
$R_{\text{work}}/R_{\text{free}}$	0.170 (0.204) / 0.192 (0.233)	0.170 (0.238) / 0.203 (0.269)
No. atoms Protein / Ligand / Water	10253 / 284 / 765	20488 / 484 / 977
B-factors (Å <sup>2</sup> ) Protein / Ligand / Ion / Water	25.2 / 28.7 / 32.5	31.5 / 31.0 / 32.4
Rms deviation from ideal geometry Bond lengths (Å) / angles (°)	0.011 / 1.549	0.010 / 1.548
Ramachandran plot Preferred / Allowed / Outliers (%)	96.1 / 3.2 / 0.7	94.7 / 4.6 / 0.7
<b>PDB code</b>	7DBJ	7DBK

Values in parentheses indicate the highest-resolution shell.